Solar Storms, Supernovae and Anomalies in Radiocarbon Production

Research performed at CIO
EES MSc-project

Talia Abi Nassif
EES 2021-2022

Master Programme Energy and Environmental Sciences, University of Groningen

university of groningen / faculty of science and engineering / energy and sustainability research institute groningen

Research report of Talia Abi Nassif

Report: EES-2022-539

Supervised by:
M.W. Dee (RUG), Center for Isotope Research (CIO)

University of Groningen
Energy and Sustainability Research Institute Groningen, ESRIG

Nijenborgh 6
9747 AG Groningen
T: 050 - 363 4760
W: www.rug.nl/research/esrig

List of contents

Abstract

Radiocarbon analysis is one of the most reliable tools for detecting cosmic events that happened during Earth's history. In fact, it has led to the discovery of two distinct spikes in radiocarbon (^{14}C), which were caused by bursts of cosmic radiation, that we now call Miyake Events. These occurred in AD 775 and AD 994, but scientists have been trying to locate more of them using $^{14}C/^{12}C$ data measured on tree-ring samples of known growth year by Accelerator Mass Spectrometry (AMS). The aim of this research is to investigate the existence of two Miyake Event candidates in AD 1054 and AD 1279. This is done by preparing batches of tree-rings spanning nine years, in duplicate, as well as some quality control references. The results are compared with the annual radiocarbon database of ETH Zurich, as well as data from other published studies. Our results showed remarkable agreement, both internally and in comparison, with the published data sets. However, they strongly negate the claim that cosmic events occurred in AD 1054 an AD 1279. This finding has important implications for the hazard posed by cosmic events, as well as possibilities for their mitigation.

Acknowledgements

I would like to thank Prof. Michael Dee for always being available to help me, for giving me great and interesting insights to the radiocarbon community, which have been so helpful in writing this thesis. I want to thank him for being very organized, which was of great help while performing laboratory experiments that needed a lot of precision. In addition, he is always so understanding and supportive in any aspect concerning my work and for that I am very grateful.

I would also like to thank PhD student Pinar Erdil for teaching me the tips and tricks of the laboratory procedures, and always being available for questions.

Finally, I want to thank Andrea Scifo, Sanne Palstra, Bert Kers and all other CIO staff that contributed to the completion of this project.

It was an amazing experience, thank you all so much.

List of abbreviations

- Accelerator Mass Spectrometry: (AMS)
- Acid-Base-Acid: (ABA)
- Bleach ($NaClO_2$)
- Demineralized Water: (DW)
- Gamma Ray Burst: (GRB)
- Hydrochloric Acid (HCl)
- International Sunspot Number (ISN)
- Radiocarbon: Carbon-14 (^{14}C)
- Room Temperature (RT)
- Sodium Hydroxide (NaOH)
- Solar Particle Event: (SPE)
- Supernova Remnant (SNR)
- Supernova: (SN)

Solar Storms, Supernovae, and Anomalies in Radiocarbon Production

Introduction

Isotope definition

Carbon is one of the most essential elements of all organic material. In fact, it is present in the atmosphere, in the ocean, in Earth's crust and in all living organisms (NASA GMS, 2009). Carbon has three isotopes, which means that the number of protons in the nucleus stays the same, only the number of neutrons will vary (Global Monitoring Laboratory, 2021). As a matter of fact, Carbon-12 (^{12}C) has 6 protons and 6 neutrons, ^{13}C has 6 protons and 7 neutrons, and finally ^{14}C has 6 protons and 8 neutrons. The first two isotopes are stable and constitute the majority of carbon on Earth: ^{12}C represents an abundance of 98.9%, and ^{13}C of 1.1% (Global Monitoring Laboratory, 2021). The third carbon isotope ^{14}C is very rare, as well as radioactive, and is therefore called radiocarbon (Global Monitoring Laboratory, 2021), which is the key isotope in this research project.

Natural production of radiocarbon

Natural radiocarbon is produced in the Earth's upper atmosphere (De Jonge., 1981; Jull et al., 2014). Its production depends on the level of solar activity (sunspot number), the strength of the geomagnetic field, and the flux of galactic cosmic rays that reach the Earth (Brehm et al., 2021). These rays hit our atmosphere at an incredible rate of 1000 particles/m^2/s (Gaisser et al., 2016). The flux of these cosmic rays consists of different ionized nuclei distinguished by their high energies: around 90% of them are protons, 9% are Helium nuclei (**α**-particles), and the remaining 1% are heavier nuclei (Gaisser et al., 2016). In fact, some nuclei of elements as heavy as lead have already been measured by the NASA Goddard Space Flight Center (2017).
When these cosmic rays interfere with Earth's atmosphere - which is predominantly composed of nitrogen molecules - the neutrons released will slow down as they scatter and collide with nitrogen, consequently producing radiocarbon in a secondary reaction (Güttler et al., 2015; Cannon P.S., 2013), as portrayed by the equation below:

$$^{14}N\ (n,\ p)\ ^{14}C \qquad [1]$$

This nuclear reaction indicates that one neutron will react with one nitrogen atom. This will lead to 7 protons and 8 neutrons inside the nitrogen nucleus in the first stage of the reaction. By releasing a proton, the nucleus now consists of 6 protons (indicating the carbon element), and 8 neutrons indicating the ^{14}C isotope called radiocarbon (Brothwell et al., 2004). Other reactions such as $^{16}O(p,\ 3p)^{14}C$, $^{16}O(n,\ 2pn)^{14}C$, can also produce radiocarbon but they are much less

common (De Jong., 1981; Dee et al., 2017). That being said, as soon as radiocarbon atoms are formed in the stratosphere, they are quickly oxidized and become part of the carbon cycle (Kovaltsov et al., 2012).

The Carbon Cycle

Carbon isotopes, and their respective compounds, take part in a complex system called the carbon cycle. This cycle is made up of reservoirs (land, ocean, atmosphere, plants) representing where the carbon atoms reside at any one point in time. Each reservoir contains a steady concentration of carbon, and when one reservoir gets perturbed by a shift in its carbon concentration, then other reservoirs will get affected accordingly (Riebeek H., 2011; Kitagawa et al, 1998). Some examples of reservoir perturbations are: the burning of fossil fuels leading to an excess of ^{12}C in the atmosphere (Riebeek H, .2011), deforestation leading to a smaller number of plants performing the photosynthesis phenomenon which would drastically affect two or more reservoirs (Riebeek H, .2011), and also particle bombardment either from space or nuclear bomb tests which both would lead to an excess of radiocarbon in the atmosphere (Scharpenseel, H., 1989).

To better illustrate the relationship of the carbon cycle with this research, radiocarbon travels through Earth's upper atmosphere by stratospheric winds until it becomes well mixed in the air and, after progressing through the troposphere, it reaches Earth's surface (Brothwell et al., 2004). There, the majority of radiocarbon is absorbed by the oceans, whereas only 1 to 2 percent of the atmospheric radiocarbon gets absorbed by plants through photosynthesis (Brothwell et al., 2004).

When plants absorb carbon dioxide (CO_2), they initially favor the lighter molecule $^{12}CO_2$ (i.e. containing carbon-12), then $^{13}CO_2$ and finally $^{14}CO_2$ (Ramsey, 2008). All of those carbon atoms will contribute, through photosynthesis, to the formation of glucose which is stored in tree rings. Looking deeper, we find that inside those tree rings is the sum of a chain of glucose molecules called cellulose (Sensuła et al., 2011). This is important for this research because radiocarbon stored in cellulose will stay intact for thousands of years in some extreme conditions (Sjostrom E., 1981) like high altitudes, peat bogs, and alluvial sediments (Kromer, 2009). In fact, because of the chemical inertness, the fibrous structure and the strong hydrogen bonds of cellulose, it has a high tensile strength and is insoluble in most solvents (Sjostrom E., 1981). This is extremely important in radiocarbon dating because cellulose in tree rings helps scientists to measure the radiocarbon content in a specific space and time, which is an excellent tool to identify the changes in the carbon cycle as well as the occurrence of cosmic events in Earth's history.

Dendrochronology and Cross-Dating

Dendrochronology is defined as the study of tree rings (Kromer B., 2009). In fact, to determine the age of a tree, two techniques can be used. The **first** one is counting the number of rings in the tree's trunk. As a matter of fact, each ring indicates one year that the tree has been alive for; so, if a tree is a hundred years of age, it would contain one hundred tree rings (Ramsey B. C., 2008). The first known record stating that a tree's rings could determine its age was first

documented by the amazing Leonardo da Vinci (Guibal, F., & Guiot, J., 2021; Bogino, S., 2014). Later on, Andrew Ellicott Douglass (A. E. Douglass), an American astronomer and archaeologist, discovered the relation between the weather on Earth and sunspots while also working on tree rings (Guibal, F., & Guiot, J., 2021; Bogino, S.. 2014). His discovery opened great opportunities in areas like climate change, fire history, ecology, archaeology and hydrology at his establishment, now called the Laboratory of Tree-Ring Research (LTRR). In fact, dendrochronology is a powerful dating method in geosciences and prehistory because it provides altitude-specific, region-specific and climate-specific dates (Kromer B., 2009). In contrast, radiocarbon dating via tree rings can indicate global measurements because of the fast mixing of CO_2 in the Earth's atmosphere (Kromer B., 2009).

The **second** technique to determine the age of a tree is called cross-dating. It is the most basic principle of dendrochronology because it ensures that each individual tree ring is assigned its exact year of formation (Douglass A. E., 1941). It is done by matching patterns of wide and narrow rings between (a) cores of the same tree, and (b) between trees from different locations (Douglass A. E., 1941).

Radiocarbon Dating

When investigating the radiocarbon content of tree rings, measuring techniques have varied through the years. With the development of the accelerator mass spectrometer (AMS), radiocarbon dating has proven to be an important and efficient tool for chronological studies for the past 50,000 years (Hackens T., 1995). In fact, one of the major advantages of the accelerator is the possibility of dating extremely small chemical fractions of samples. In fact, samples containing less than 1mg of carbon can be dated (Hackens T., 1995). Moreover, radiocarbon measurements via the Tandem AMS have improved through the years to gain better precision in counting because dating radiocarbon should be really precise because natural levels of $^{14}C/^{12}C$ are in the range of approximately 10^{-12} (Rubin et al., 1963; Hackens T., 1995). In fact, radiocarbon dating investigates the ratio of $^{14}C/^{12}C$ in the atmosphere relative to an international standard, and corrected for radioactive decay; thus, it really provides the rise and fall in annual radiocarbon concentrations in the atmosphere.

To measure this $^{14}C/^{12}C$ ratio inside the accelerator, the atoms of the samples are converted into negative ions inside the ion source, in contrast with the conventional AMS which converts them to positive ions (Hackens T., 1995). This step is beneficial to separate the stable masss-14 nitrogen isotope which cannot form a stable negative ion (Hackens T., 1995). After stripping the ions with Helium gas, they turn into positive ions, and get accelerated a second time. Finally, they get separated relative to their mass and counted in an ion detector right before the mass analysis, which represents the final results (Hackens T., 1995).

Miyake Events

Scientists have been trying, for years, to understand the relation between some cosmic events and the carbon cycle on Earth. In fact, in 2012, Fusa Miyake discovered in Japanese tree rings a massive spike in $\Delta^{14}C$ of approximately 12‰ that dated back to AD 775 (Miyake et al., 2012). Fusa Miyake also found another spike, slightly smaller, in AD 994 (Miyake et al., 2013). Those single-year anomalies in radiocarbon are the result of an intense burst of radiation from space (Dee et al., 2017). This was deduced because, as described in previous sections, the only known natural pathway of radiocarbon production is via cosmic ray bombardment. In fact, no terrestrial phenomenon like a volcanic eruption (Craig H.,1957) or some land use change could explain the 12‰ increase in radiocarbon, thus scientists are looking for answers from the cosmos. So, slightly after Miyake's discoveries were published, many labs around the world like in Germany (Usoskin et al., 2013), the USA and Russia (Jull et al., 2014), New Zealand (Güttler et al., 2015) and more, managed to reproduce those measurements as shown in *Figure 1* below.

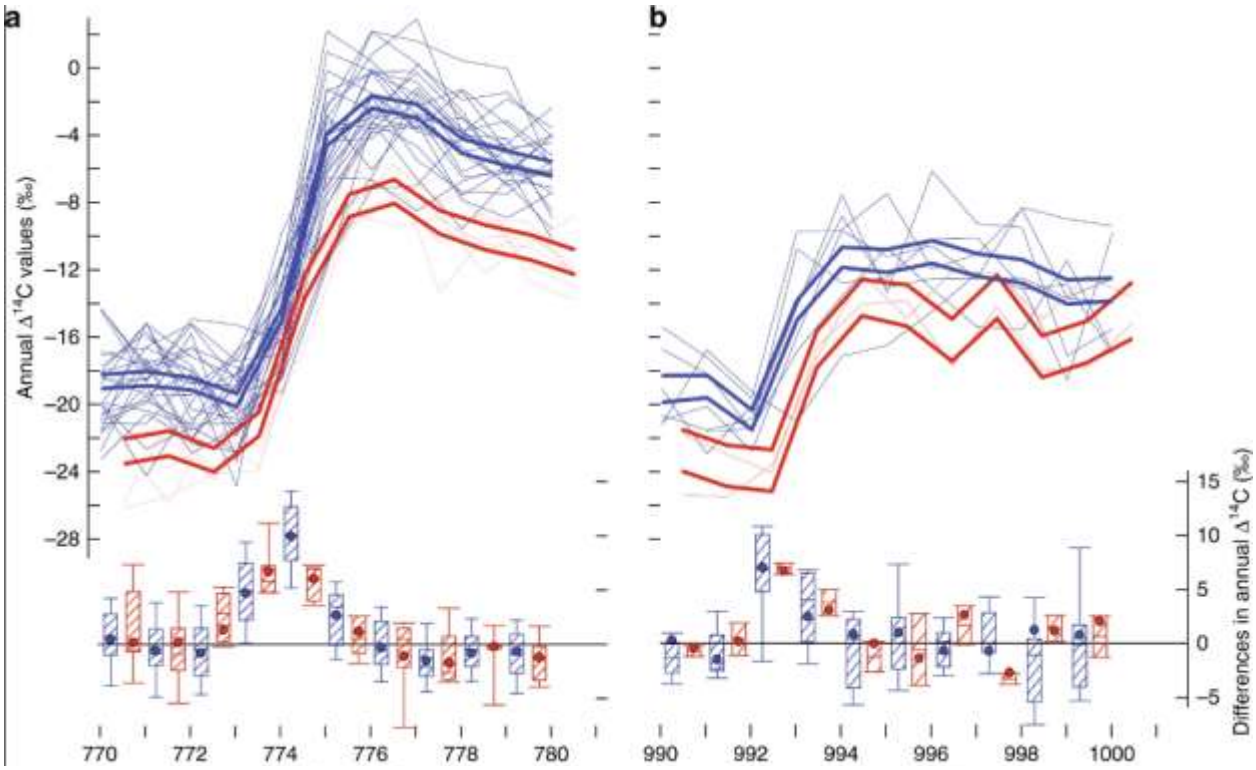

Figure 1: These two graphs represent measurements from seven different laboratories, who investigated the spikes that Fusa Miyake found in 775 (a) and 994 (b) (Büntgen et al., 2018). The results are consistent with a massive and rapid annual peak in Δ14C, which led to those anomalies being named Miyake Events. The figure was reproduced in its entirety from Büntgen et al., 2018

One important thing to point out is that cosmic rays get deflected by different magnetic fields on their journey to Earth, which makes the search for their origin very complicated (NASA Goddard Space Flight Center, 2017). That is due to the charge of those cosmic rays: they are either positively or negatively charged, which makes them sensitive to the magnetic fields of the galaxy, the heliosphere, and the Earth; thus, their path to Earth is wildly unpredictable as illustrated in blue in *Figure 2* below, whereas light, a form of gamma rays (in purple), travels

directly to us, which helps us point to some historical sighting from space like supernovae for instance (NASA Goddard Space Flight Center, 2017).

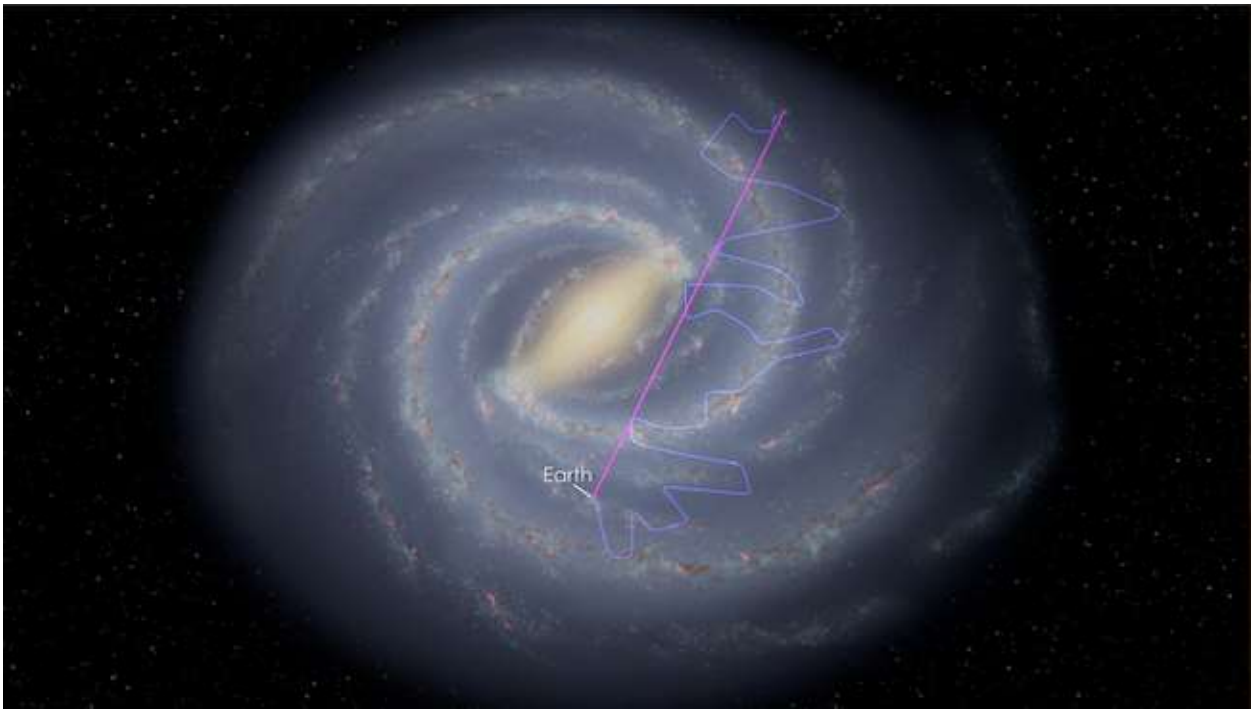

Figure 2: The purple line indicates light passing through space and reaching Earth with no deviation, whereas the blue line represents cosmic rays travelling through space and being redirected by multiple magnetic fields until finally reaching the Earth (Figure reproduced in its entirety from NASA Goddard Space Flight Center, 2017).

Origin Theories of Miyake Events

Finding the source of the Miyake Events is one of the most fundamental questions in cosmic-ray physics today. Although the cosmic particles that have entered our atmosphere cannot be traced back (Scifo et al., 2019), some theories have already come to light concerning the origin of Miyake Events, e.g. the Sun, a supernova, a comet, or gamma-ray bursts (GRBs) from magnetars and pulsars. And even though their origin is still unknown, it is likely that most cosmic rays come from outside the solar system, but from within the galaxy (Gaisser et al., 2016). If the origin question gets answered, it would shed more light on the occurrence frequency of such events, their magnitude, and the consequences that we need to be able to face.

First, let's talk about solar origin. The sun doesn't always shine at the same rate, it goes through periods of high solar activity (an increased number of sunspots) and low solar activity (a decreased number of sunspots), which results in different concentrations of cosmic rays being ejected and propelled in space, and sometimes directly towards Earth.

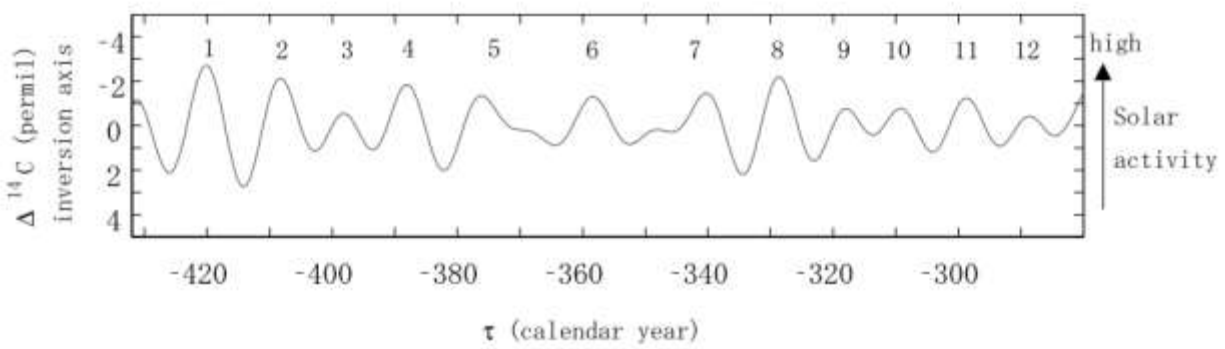

Figure 3: Δ14C fluctuates between positive and negative values depending on an increase or decrease in solar activity. As a matter of fact, a lower solar activity will result in a shallower geomagnetic field, thus leading to more particles entering the atmosphere, and consequently more radiocarbon being produced. This can be seen in Figure 3 as a higher solar activity leads to negative values of $\Delta^{14}C$ and a lower solar activity leads to positive $\Delta^{14}C$ values (Figure reproduced in its entirety by Nagaya et al., 2012).

As indicated in the measurements from Nagaya et al. (2012), radiocarbon production is anticorrelated with solar activity. That means that the higher the sun's activity is, the less radiocarbon is produced on Earth. This is due to the low-energy cosmic rays reaching the Earth when the heliomagnetic activity is low. The much larger flux of low-energy galactic cosmic rays (still many orders of magnitude more energetic than solar cosmic rays) that reach Earth causes the geomagnetic field to become shallower, thus allowing low-energy cosmic rays to enter our atmosphere (Nagaya et al., 2012). Another distinct relationship that was found between radiocarbon production and the sun's activity is an 11-year cycle called the Schwabe cycle. It is a variation of the average number of sunspots on the Sun (Schwabe S.H., 1843). The study by Scifo et al. (2019) indicates that both AD 775 and AD 994 Events as well as the Carrington Event all seem to have occurred during the most active phases of the Schwabe cycle, which is supporting a solar origin. The Carrington Event occurred in AD 1859 and is the solar storm that caused the largest geomagnetic storm ever detected on Earth (Cannon P.S., 2013; Scifo et al., 2019).

Indeed, when we say that the sun might be the cause of these Miyake Events, we are talking about some massive solar flares, or solar particle events (SPEs) which would burst out energetic particles like electrons, protons, **α**-particles, and other heavier particles into interplanetary space (NASA Space Radiation Analysis Group, 2020). These particles are accelerated to a point near relativistic speeds by the shock waves preceding fast coronal mass ejections CMEs (NASA Space Radiation Analysis Group, 2020), which are massive expulsions of plasma and magnetic field from the Sun's corona (NOAA, 2022). This leads to particles reaching Earth within only tens of minutes, whereas the low-energy solar cosmic rays will arrive within about a day (NASA Space Radiation Analysis Group, 2020). Some suggest that the hypothesized SPE that would cause such a big 12‰ rise in the first discovered Miyake Event in AD 775 would have to be 45 times stronger than the most intense high-energy SPE observed on February 23rd, 1956 (Usoskin et al., 2020), or 5 times as energetic as the Carrington Event (Cliver et al., 2014). In addition, the Carrington Event also led to a global auroral display, about which there is no record of dating back to AD 994 and AD 775 (Wang et al., 2019; Chai et al., 2015). Additionally, if Miyake Events were caused by an SPE slightly larger than the Carrington Event of 1859 as Usoskin (2013) claims,

then the three events would all have a similar trend, which is not the case as seen in *Figure 4* below.

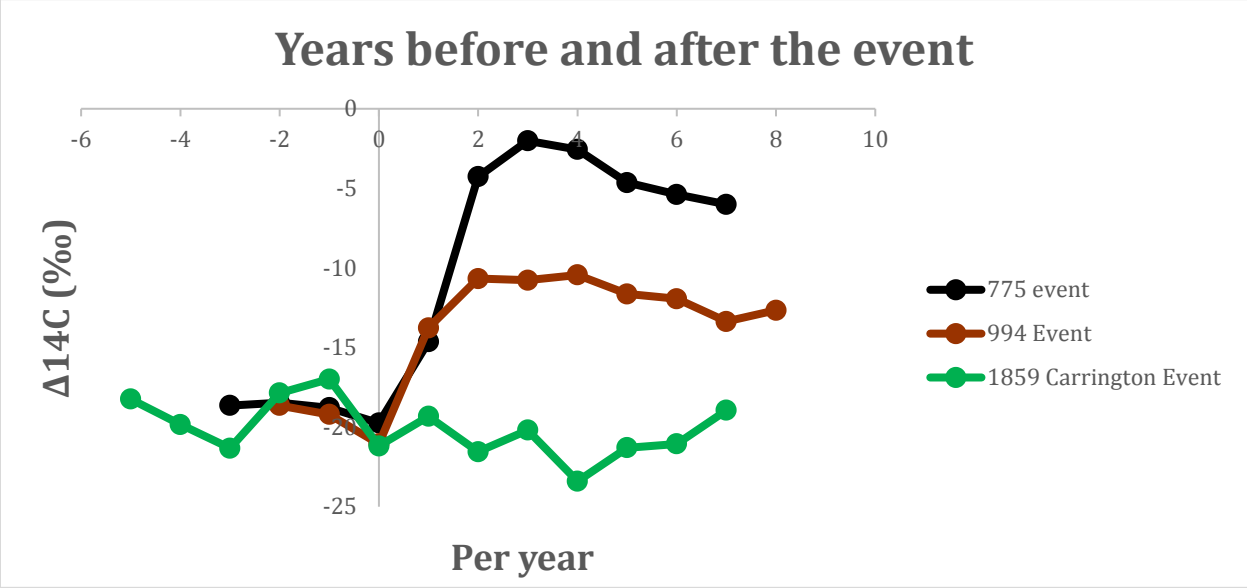

Figure 4: The graph plotted above contains the measured Δ14C of both Miyake Events that took place in AD 775 and AD 994, as well as the measured Δ14C of the energetic solar phenomenon: The Carrington Event. As apparent above, the Carrington data show no spike at the time or after the event compared to the other two.

Attributing Miyake Events to the **Sun** is however not straightforward. In fact, this explanation has both supporters and opponents because we already know of the previously mentioned anti-correlation between the Sun and radiocarbon production (Stuiver M., 1961; Damon et al., 1973; Damon et al., 1986); we also haven't witnessed a rise in radiocarbon production during the Carrington Event (which was definitely caused by the Sun); hence why some analysis still contradict the claim for a solar origin for Miyake Events (Hambaryan, V. V., & Neuhäuser, R. (2013); Pavlov et al., 2013). Moreover, by analyzing and comparing the energetics and spectra of the 1956 SPE and the AD 775 Event, Cliver et al. (2014) pointed out that there were inconsistencies concerning the occurrence-probability distribution for SPEs, which speaks against a solar origin (Wang et al., 2019). On the other hand, intense SPEs or interplanetary coronal mass ejections (ICMEs) have been suggested as a cause for Miyake Events by Melott and Thomas 2012; Thomas et al. 2013; Usoskin et al. 2013; Güttler et al. 2015; Mekhaldi et al. 2015.

Recent studies suggest the occurrence frequency of superflares on solar-type stars (although superflares have not yet been observed on our sun (Shibata et al., 2013)) is around 1 in 3000 years, which is too low for Miyake Events (Wang et al., 2019). Last but not least, it is actually still debated if the Sun can even produce such large proton events that would increase $\Delta^{14}C$ by 12‰ in 1 year (Wang et al., 2019; Miyake et al., 2012; Hambaryan and Neühauser 2013; Pavlov et al. 2013).

The second theory concerning the origin of Miyake Events is a **supernova** (SN), i.e. a star exploding and emitting very bright light (gamma-ray flux), highly-energetic particles, and a supernova remnant that will last for thousands and thousands of years (Dee et al., 2017). In fact, many types of supernovae remnants exist and their luminosities vary widely. We expect that galactic SN happen at a rate of approximately 1 or 2 per century, which leads to believe that a lot of past SN have gone undetected (Dee et al., 2017). Considering the biggest Miyake Events, which happened in CE 775 or CE 994, there was no record of a SN in historical observations, nor a supernova remnant (SNR) relevant to either of those dates (Güttler et al., 2015; Dee et al., 2017), unless the supernova was hidden behind a dense interstellar cloud of gas and dust as propsed by Pavlov et al (2014). But can supernovae really be responsible for such massive spikes in radiocarbon records?
A study by Menjo et al. (2005) could not discern any significant uplift for SN1006; another study by Dee et al. (2017) failed to detect a radiocarbon anomaly for SN1054 that left behind the famous Crab Nebula, or any of the five other historical supernovae SN185, SN1572 and SN1604 (Dee et al., 2017). Overall, the gamma ray flux emitted from a supernova could potentially increase radiocarbon production but it may be too low to be detectable by this approach (Dee et al., 2017), especially with the 4-6‰ fluctuations of the Schwabe Cycle (Menjo et al., 2005) and noise-induced errors during the measurements.

The third theory concerning the origin of the Miyake Events is a **comet,** travelling so close to Earth that it spread radiocarbon in the atmosphere, causing a 12‰ rise in AD 775. As a matter of fact, comets get enriched in radiocarbon when bombarded by cosmic rays on their way to us, thus as it burns through Earth's atmosphere, it would produce carbon-14 and beryllium-10 (another radionuclide) by nuclear reactions (Liu et al., 2014). It is interesting to point out that on January 17th, AD 773, a comet sighting from the Orion constellation was recorded in several Chinese archives, along with "dust rain" from the day before, which implies that a significant amount of cometary material was added to the atmosphere. These two phenomena were most probably linked to each other; however, no source other than the Chinese records has mentioned either of these so far. Considering the comet appeared in January 773, and the residence time of radiocarbon in the atmosphere, it would have taken those radiocarbon atoms approximately a whole year to reach the surface and enter tree rings through photosynthesis (Liu et al., 2014). As for the AD 994 event, no records of a comet sighting were found, but that doesn't reject the whole theory because the comet could have appeared above a desert or the pacific, also left with no witnesses. Now there have been some counter arguments for the comet theory. For instance, Usoskin predicted in 2015 that the comet dimensions would need to be massively bigger than previously estimated.

A little less common, but definitely worth mentioning, are **gamma ray bursts** (GRBs). In fact, gamma rays are high-energy light beams, that could cause atoms to break up and release neutrons via photonuclear reactions. Furthermore, GRBs are the most powerful explosions in the cosmos, to the point where they can be detected across billions of light-years (Reddy F., 2021). The short GRBs last for only about two seconds and they occur when a pair of orbiting neutron stars, both the crushed remnants of supernovae, spiral and merge into each other (Reddy F., 2021). To elaborate, there are different types of neutron stars that could emit highly energetic

GRBs, i.e. pulsars and magnetars. **Pulsars** are highly magnetized neutron stars. They emit a large beam of electromagnetic radiation (gamma rays) which, by interacting with Earth's atmosphere, will produce radiocarbon and cause a rise in tree-ring radiocarbon (Wang et al., 2019); whereas **magnetars** are neutron stars with the strongest-known magnetic fields (Reddy F., 2021). They produce violent transient and radiative phenomena like soft gamma-ray bursts (GRBs) and giant flares at a small rate of less than $10^{-3}.yr^{-1}$ for the Milky Way galaxy (Wang et al., 2019). For the AD 775 Event, Hambaryan and Neuhäuser (2013) estimate that a short GRB in our galaxy would be consistent with the energy levels of particles needed for Miyake Events, consistent with the production rates of carbon-14 and beryllium-10 seen over these events, and consistent with the absence of evidence for a SN and a SNR. Finally, if a short GRB would be around 1 to 4 kpc far from the Earth, no extinction event would occur on Earth while being sufficiently powerful that its γ-rays will produce a meaningful rise in $\Delta^{14}C$ (Güttler et al., 2015).

Hazards of cosmic events

Looking back on the biggest Miyake Event discovered so far (AD 775), society back then wasn't dependent on technology, i.e. GPS systems, satellites or even smartphones, but should these events happen now (or in 20 years), they would be disastrous to modern technological civilization (Hapgood., 2012), and they would potentially destroy Earth-bound electrical infrastructure (Dee et al., 2017; Brehm et al., 2021) which would take between weeks and months to repair (Cannon P.S., 2013). Extreme cosmic events would also cause data upsets, component damage, and even lead to false commands on satellites (Cannon P.S., 2013). In addition, if the true origin were not the Sun but gamma rays from other sources in the universe, studies by Wang et al. (2019) suggest that high-energy photon emissions, or pulsar bursts, could deplete the ozone layer and affect atmospheric mixing. Some mitigation possibilities have been discussed later on in this study.

Research Questions

In recent findings, two new candidates for the Miyake Events, AD 1054 and AD 1279, were proposed by Brehm et al. (2021), claiming that they would be extremely harmful to the extraterrestrial electronic infrastructure being used today e.g. satellites, aircrafts as well as GPS systems (Bolles, 2021). A lot of questions arise like: How real are those candidates? How many more Miyake Events will we find? Can they actually be of help in situating historical archives exactly in time by ^{14}C spike-matching methods (Hakozaki et al., 2018)? What challenges will we face? And what consequences will they have on our technological society of today?

With the help of the team at the CIO, Groningen, I will try to answer some of those questions. Henceforth, I prepared and measured batches of 9-year samples for each event period, along with a set of duplicates for each date, and two known-age samples from one of the kitchens in Windsor Castle for quality control purposes, i.e. to confirm the validity of my results.

It is my expectation that this research project will end in one of three ways:

1. The batch of samples will not show a $\Delta^{14}C$ peak, indicating that no detectable cosmic phenomenon happened in the time period measured.
2. The batch of samples will show a peak in $\Delta^{14}C$, hence proving that an increase of thermal neutrons in the atmosphere occurred as a result of cosmic ray bombardment in the time period measured.
3. The batch of samples will show a peak in $\Delta^{14}C$ but with a different shape and amplitude than the previously validated Miyake Events, potentially indicating a different source, or kind of event, than AD 775 and AD 994 Events.

Experimental Methods

Sample treatment and pretreatment

Samples

For this study, all tree rings are known-aged samples between AD 1049 and AD 1057, AD 1275 and AD 1283, as well as two Windsor Castle samples both dating back to AD 1503.

Physical pretreatment

The wood samples are first physically prepared, which means they are cleaned from any contaminants like cotton from packaging, glue, or anything that might contain carbon and have an impact on the extracted carbon and the results of this experiment.

After making sure the wood samples are clean and entered carefully in the database, they are cut into thin pieces of around 50mg of wood for each year and then respectively labeled. As a first experiment (for the first candidate event), the total number of samples is 19, i.e. 9 wood samples from the years AD 1275 to AD 1283, 9 duplicate samples, and a known-age (AD 1503) wood sample from Windsor Castle. The second experiment also consists of 18 duplicates from the year AD 1049 to AD 1057 and another known-age sample from Windsor Castle. This is done as a way to validate the measurements and minimize the error margin in the experiment.

Chemical pretreatment

Each tree sample goes through an intensified aqueous pretreatment, in this case called ABA, which stands for Acid-Base-Acid, to extract the (α)-cellulose from the wood. (α)-cellulose is a common term for cellulosic product rich in long chains, as opposed to hemicellulose which tends to contain shorter chains and free sugars such as sucrose and fructose (Machmudah et al., 2017). This pretreatment starts with a strong acid (HCl, 5.47% w/vol (1.5 M)), at 80℃ and for 20 minutes. After the 20 minutes have ended, the samples are rinsed three times with Demineralized-Water or Demi-Water (DW). The next step consists of leaving the samples in a strong base for an hour. They are placed under N_2 atmosphere and ultrasonicated for 60 minutes at room temperature (RT), while submerged in NaOH (17.5% w/vol). After leaving the samples for an hour, they are decanted and rinsed five times again with (DW). The next step in the ABA pretreatment is pouring the acid again on the samples (HCl, 5.47% w/vol) for 20 minutes at a temperature of 80℃, which is similar to the first step. The samples are rinsed three times with DW and are ready to be left in bleach (aqueous oxidant) overnight. This aqueous oxidation step consists of leaving them in $NaClO_2$ (1.5% w/vol in HCl 0.06 M) in a dry-block heater at 80℃ for 16 hours. After those 16 hours, the $NaClO_2$ solution is prepared and added again and the samples are left for 4 hours under the fresh acidified oxidant (maximum time in bleach is 20 hours). The last step of the (α)-cellulose extraction is rinsing the samples three times with DW and freezing them before

combusting them, graphitizing them, and measuring their radiocarbon content in the accelerator mass spectrometer (AMS) which will be discussed in the following paragraphs.

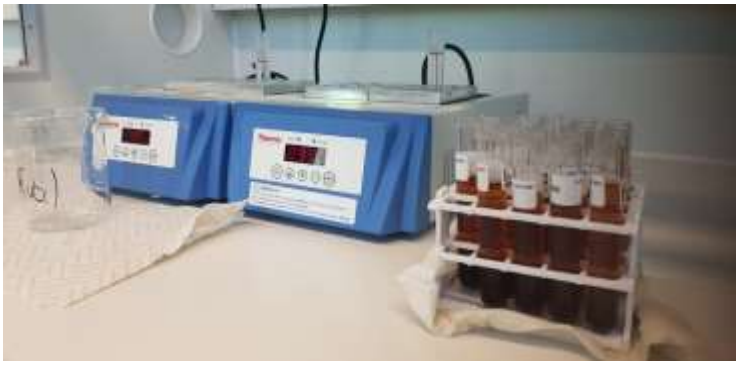

Figure 5: This picture shows all of my samples as they were being treated in acid. As seen above, the wood material is slowly degrading and its color will fade away little by little, until only the white cellulose will remain after the ABA treatment and the overnight-bleach treatment.

Combustion and Graphitization

To measure the radiocarbon concentration contained in the (α)-cellulose powder, the samples are placed in very small tin capsules (5mg is ideal for each cellulose sample taken from tree rings as seen in *Figure 6* below).

Figure 6: This picture shown above represents the annual cellulose of my first batch of samples, weighting around 5mg each, and wrapped in one or more tin capsules, ready to be combusted and graphitized before being sent to the AMS for radiocarbon measurement.

The combustion process takes place in an Elemental Analyzer (EA) coupled with an Isotope Ratio Mass Spectrometer (IRMS), which allows $\delta^{13}C$ and $\delta^{15}N$ to be determined, and an automated cryogenic collection system which will trap the carbon dioxide released into sealable glass vessels (Dee et al., 2020). After the combustion process is complete, the glass vessels are redirected to graphitization manifolds, where an Fe powder catalyst is introduced. The CO_2 from each sample is introduced and mixed with a stoichiometric excess of H_2 gas (1:2.5). The hot tube is then placed in an oven at 600°C. After drawing the water vapor from the reaction site, the samples are chilled between -15 and -20 °C using a Peltier device (Dee et al., 2020). Later on, the graphite samples are pressed into Al cathodes and placed in the ion source of the Micadas AMS. Here, all three isotopes of carbon are ionised, accelerated, and deflected by a series of magnetic and electric fields so the beams of the three isotopes become separated and can be measured independently (Hackens T., 1995).

Results and Discussion

First batch: Candidate event AD 1054

As discussed earlier, we prepared two batches of duplicates from AD 1049 to AD 1057 as well as a Windsor Castle sample for quality control. We measured the year AD 1051 three times as we got an outlier the first time, but that was not completely unpredictable. We had highly consistent results throughout, all duplicates were within 1σ error except for the sample from the very last date AD 1057, however it did pass the chi-square test. The chi-square test is the statistical method-of-choice in the radiocarbon community for the congruence of two dates. The threshold is usually taken to be 5%; so, if two samples pass the chi-square test, they are deemed to be statistically indistinguishable, and hence could represent the same sample at 95% (or 2σ) probability. The dashed line in blue (*Figure 7)* represents the year the event has been proposed to happen by Brehm et al. (2017), but the thing is that annual radiocarbon concentration is not constant, and we can see some fluctuation, probably from the Schwabe Cycle (around 4-6 ‰ Scifo et al., 2019); or noise which could add up to 5‰ in an AMS (Nagaya et al., 2012).

The results plotted below have been obtained by radiocarbon dates from the AMS which we convert to calendar years, then to $\Delta^{14}C$ using the following formulae:

$\Delta^{14}C = 1000 \times [F_m \times e^{\lambda(Y_0 - Y_C)} - 1]$ [2]

Where $F_m = e^{-kt}$ [3]

(F_m is the fraction modern, same as $F^{14}C$; and t is the ^{14}C date in BP),

$k = {}^{1}/_{8033}$; $\lambda = {}^{1}/_{8267}$, [4] and [5]

Y_0 is the year 1950 CE; whereas Y_C is the year of collection of the sample.

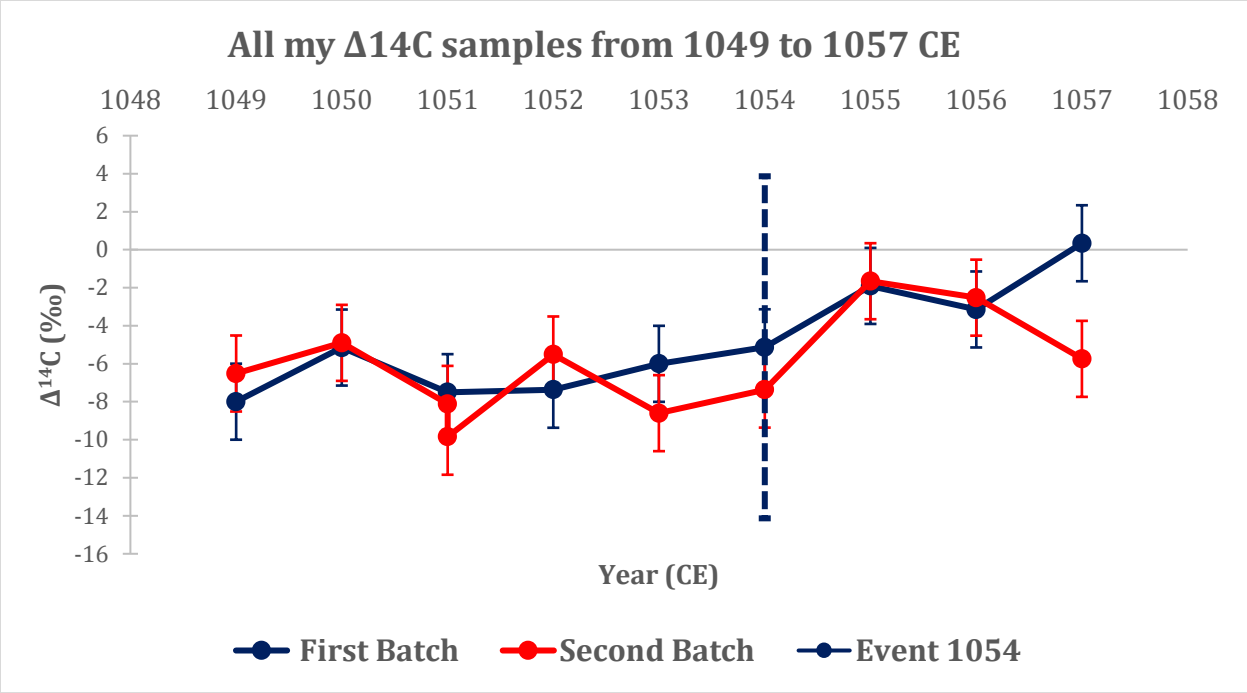

Figure 7: The tree rings dating from AD 1049 to AD 1057. The results consist of duplicates, which both are presented above, as well as a dashed line representing the candidate event AD 1054. All duplicates are located within the error bars represented in the graph which means that they are statistically indistinguishable at 1σ except AD 1057 which was still consistent at 2σ.

A small rise is evident but not one I would consider significant enough to be classified as a Miyake Event, because my results represents a rise of less than 6‰ over one year. The next step is averaging my data and comparing them to other labs, especially with ETH since they have an annual radiocarbon database for both time periods of the candidate events.

The averaged Δ14C (A_p) and averaged uncertainties (E_p) in *Table 1* are obtained by the following formulae:

$$A_p = \left(\sum_1^n A_i/{E_i}^2\right)/\left(\sum_1^n 1/{E_i}^2\right) \quad [6]$$

$$E_p = \sqrt{1/\left(\sum_1^n 1/{E_i}^2\right)} \quad [7]$$

Where A_p = Pooled average

A_i = Individual sample ^{14}C date (yr BP)

E_i = Individual sample uncertainty (yr BP)

To test the consistency of the averaged result, we run the chi-square test with A_i, A_p, and E_i:

$$T = \sum_1^n \left(A_i - A_p\right)^2/{E_i}^2 \quad [8]$$

Where T is the statistical test used to compare the means of two or more samples.
The thresholds, above which the dates will fail to be identical, and which are relevant to this study to a 95% degree of confidence are:
3.84 for 2 samples; 5.99 for 3 samples; 7.81 for 4 samples; 9.49 for 5 samples
The formulae as well as the threshold were obtained from Ward, G. K., & Wilson, S. R. (1978).

Table 1: All measured Δ14C values from my batch of duplicates (1049 - 1057), as well as the averaged Δ14C values for each date. The chi-square test was run on all measurements and they were valid (right-hand column).

	Δ14C (‰)		Δ14C (‰)	Uncertainty (‰)	T-test	Chi-square test
Year CE	**Batch 1**	**Batch 2**	**Averaged**	**Averaged**	**0<t<3.84**	**Pass/Fail**
1049	-8.00	-6.51	-7.03	2.03	0.12	Pass
1050	-5.15	-4.90	-4.90	2.0	0.00	Pass
1051	-7.50	-8.11	-8.51	1.5	0.43	Pass
		-9.84				
1052	-7.37	-5.51	-6.21	2.0	0.18	Pass
1053	-6.01	-8.60	-7.27	2.0	0.32	Pass
1054	-5.14	-7.36	-6.22	2.0	0.29	Pass
1055	-1.91	-1.66	-1.81	2.0	0.00	Pass
1056	-3.15	-2.52	-2.78	2.0	0.00	Pass
1057	0.34	-5.74	-2.82	2.0	2.63	Pass

One important thing to mention is that while my batches were being measured in the AMS, some complications occurred leading to sparking in the accelerator. Undoubtedly, the accelerator was stopped to fix the problem, but the samples had already been affected, ending up with a slightly larger error bar in the measurements. Regardless of this technical error in the AMS, my samples are still very much valid and usable, as we can validate by the Windsor Castle samples.

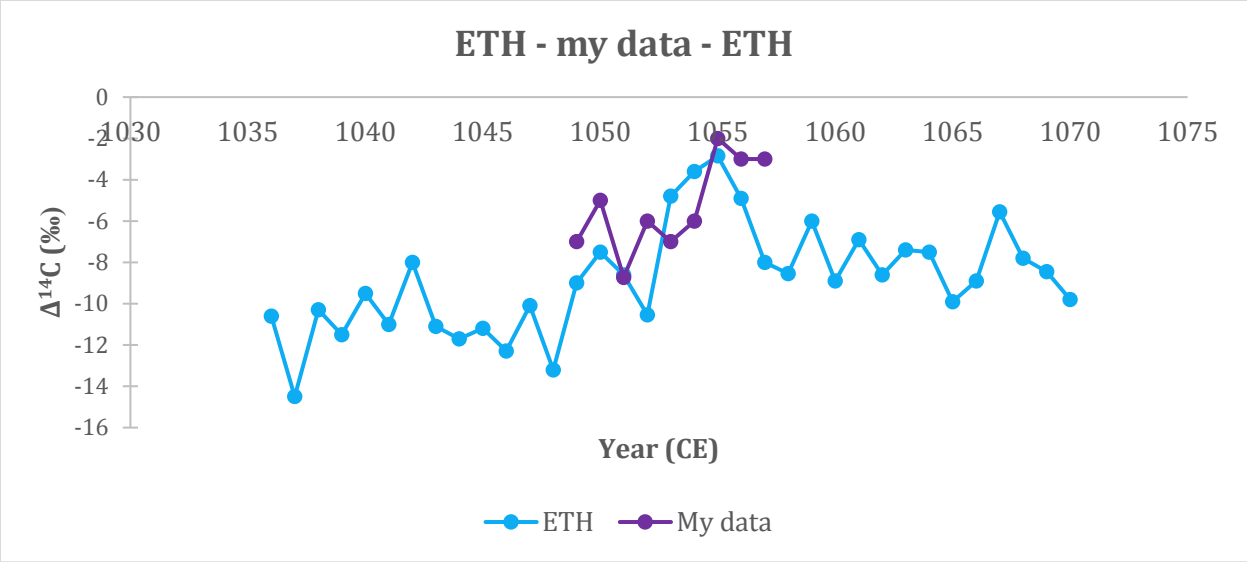

Figure 8: In this graph, before the 5.5‰ rise in AD 1052, the averaged radiocarbon content in the ETH data was lower than after the event.

Looking at the long ETH data, if a shift in a certain carbon reservoir happened (for instance the ocean uptake slowed down), then it would be a relevant cause to the slightly higher concentration of radiocarbon that we see above after AD 1055, because it does not align with other proven Miyake Event trends (Miyake et al., 2012) which experience a decline over 20 years. The *Figure* 9 below investigates and compares both my data and that of ETH on a smaller scale.

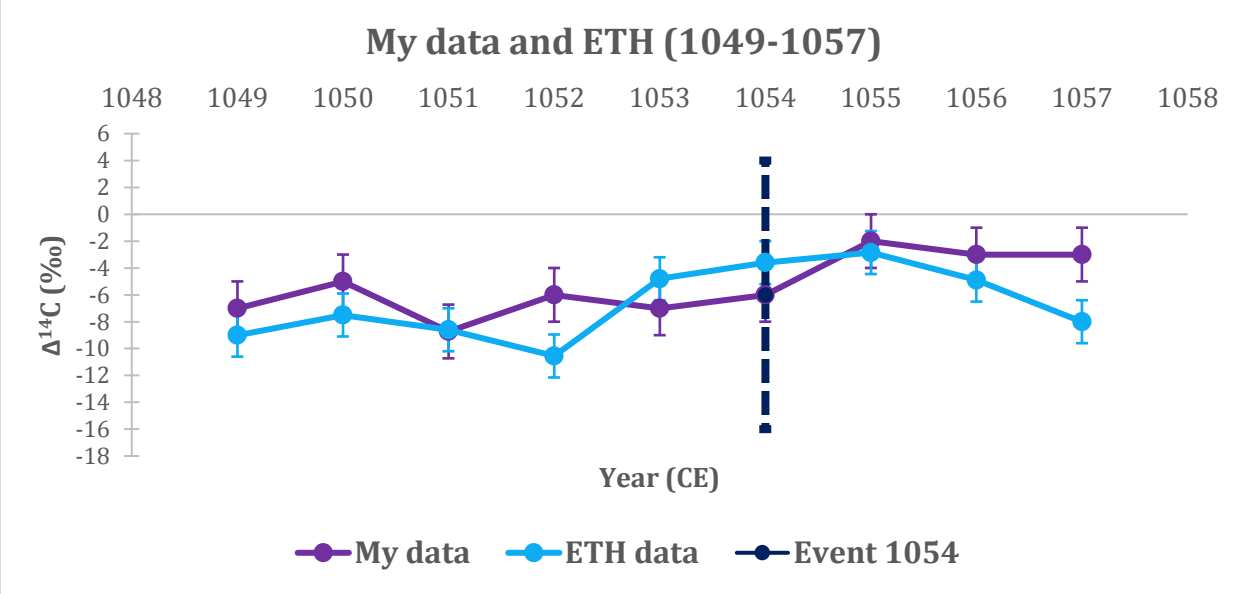

Figure 9: This graph represents my averaged data along with the averaged measurements from the ETH dataset for the years AD 1049 to AD 1057. The chi-square test was valid for all measurements except AD 1052 which was above the threshold. However, we see a consistent trend throughout the graph, and no significant rise in $\Delta^{14}C$ after AD 1054.

Examining the ETH data and my averaged data, we see a strong similarity in our results. However, ETH's data shows a small rise of 5.5‰ for AD 1052-1053, whereas my data slightly

rises two years later around AD 1054-1055. Could it be that the dendrochronology of ETH is off by a couple of years? It is very unlikely, but not impossible that a lab could make a mistake in their dendrochronological study and it is worth investigating whether their graph matches mine if it is transposed by 2 years (*Figure 10)*. We can also look deeper into that by comparing those data with other labs that measured the radiocarbon concentration over that same period of time (*Figure 11*).

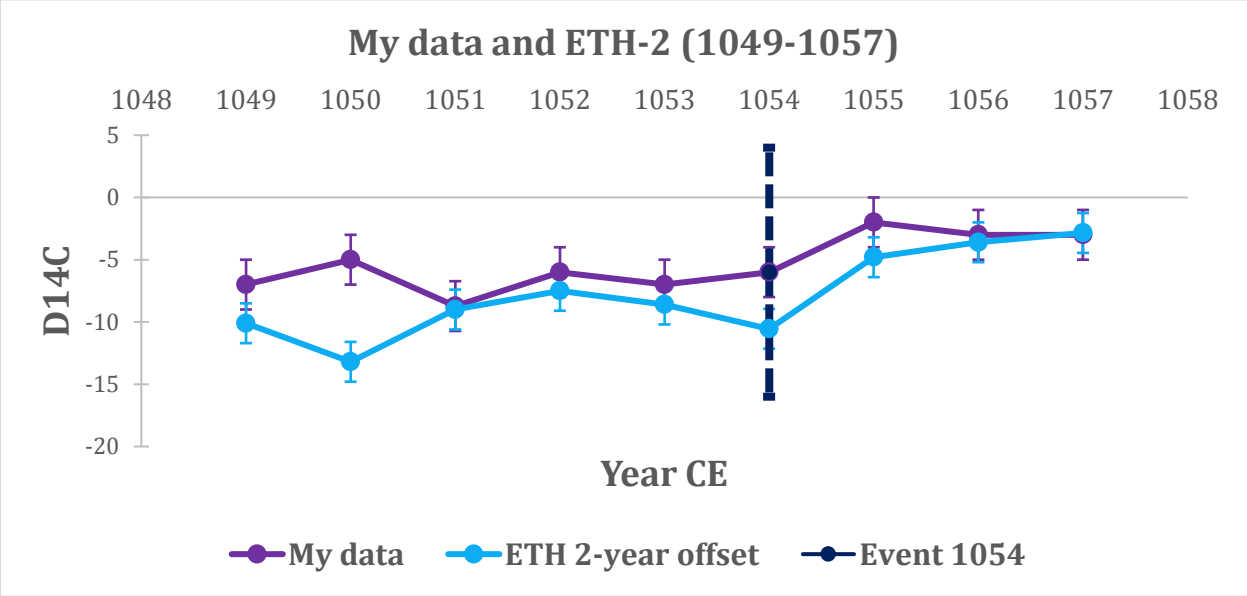

Figure 10: This graph shows the ETH data shifted forward by two years to see if the trend then matches my data better. We see that the small rise now has the same trend as mine for AD 1054, but now only seven out of nine of our data pass the chi-square test, which is a lower congruence than the original measurements.

After shifting the ETH data by two years, the trend, especially the AD 1054 rise looks more or less like my averaged data, but the chi-square test fails two samples instead of one compared to their original measurements. It is one hypothesis that ETH might have their dendro-calibration wrong, for we see a small rise but not in the same year. To explore this matter further, it is necessary to compare my results with other available data sets. We will take a look at the corresponding $\Delta^{14}C$ data from Terrasi (2020), Eastoe (2019), Menjo (2005) and compare it with ours and that of ETH. For simplicity's sake, Terrasi's years were rounded up to match the rest of the data: 1049.3 has been changed to 1049 and so on. All of the respective data is in the Appendix, along with their chi-square test results.

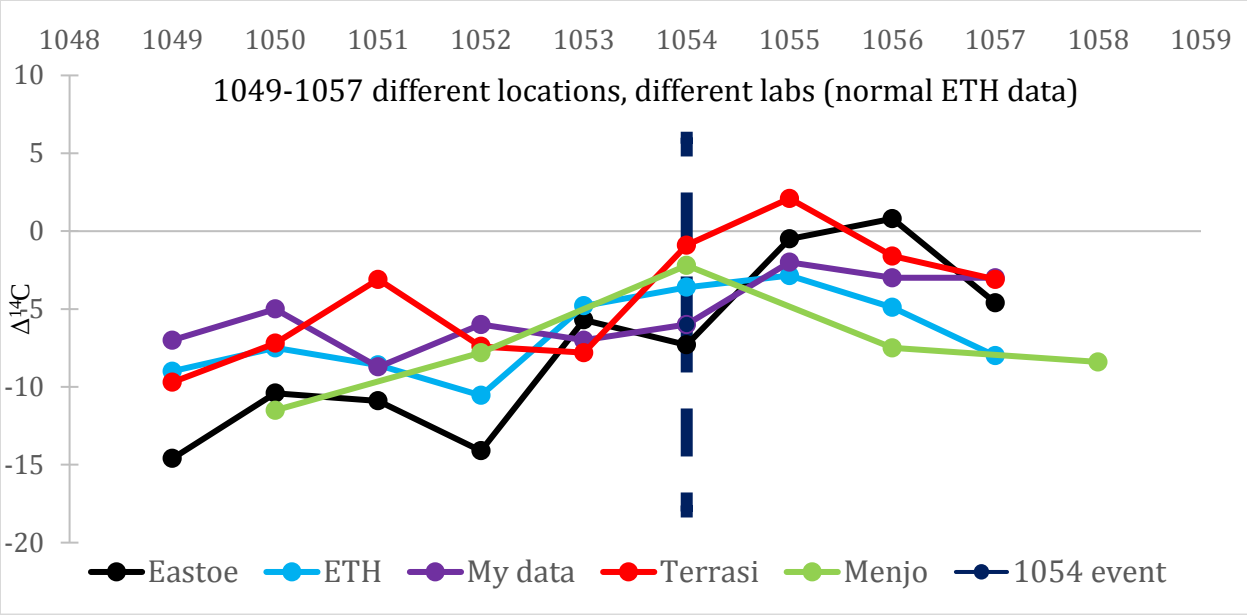

Figure 11: This graph shows different measurements of the same time period by different labs: ETH, Eastoe, Terrasi and Menjo.

Figure 11 includes data from five different labs. Eastoe's data (black) is a little scattered compared to the rest. ETH (light blue) shows a rise in AD 1052 similar in shape to mine (purple) at AD 1054. Menjo's data (green) is relatively close to mine, as well as that of Terrasi (red), which passed the chi-square test when they were running against mine. My averaged data is located in the middle of all other measurements, which would be interpreted as a consistent job. For all the data however, there is no pronounced spike that goes over 6‰ for any year. Overall, all patterns could be interpreted as noise, natural phenomena like volcanic, oceanic, land use activity that may have perturbed the carbon reservoirs; or even it might be caused by the fluctuations of the Schwabe cycle.

So, no spike similar to previously proven Miyake Events has been measured from the first batch dating from AD 1049 to 1057 in any of the labs previously mentioned. The small rise detected could be anything from noise, natural activity, or even the Schwabe cycle. Indeed, looking at all the rises and falls of the radiocarbon measurements, there is no compelling evidence which proves that only the AD 1054 rise should be interpreted as a Miyake Event and not any other spike.

Second batch: Candidate event AD 1279

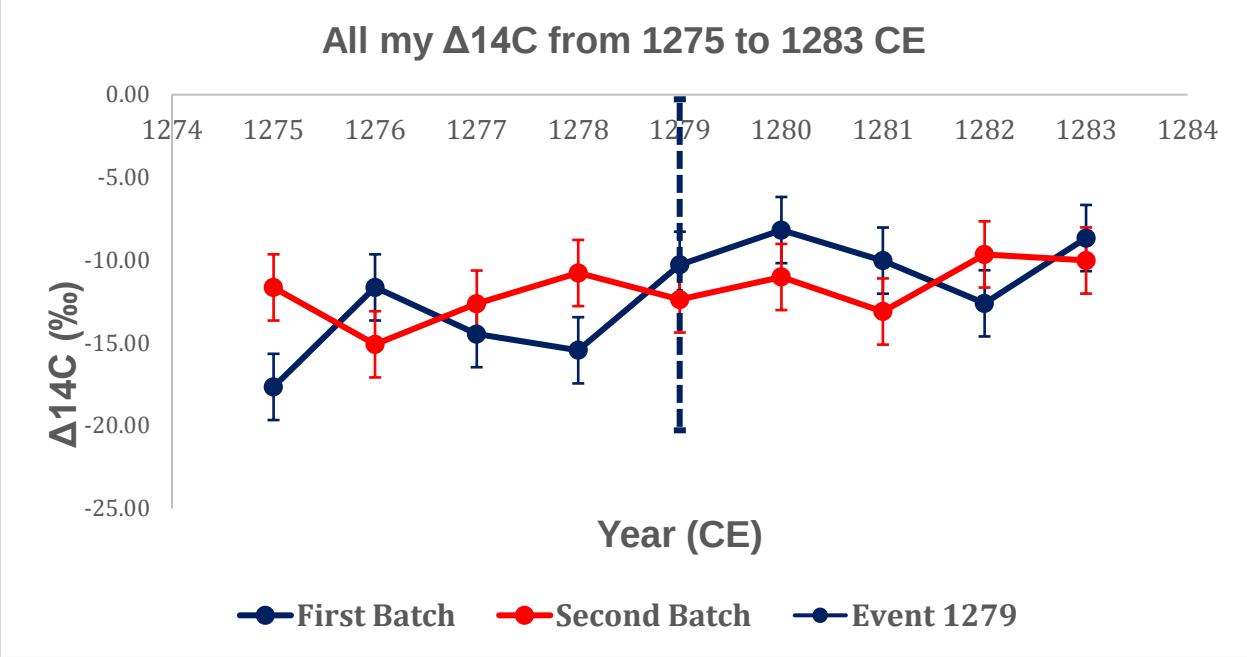

Figure 12: In this graph, all duplicates are shown for the period AD 1275-1283. The blue dashed line in the year AD 1279 indicates the year in which the event theoretically took place.

For these duplicates, all data passed the chi-square test, which means that they are statistically indistinguishable at 1σ. No significant spike above 6‰ was measured in any year during that period, even the blue rise in AD 1278-1279 is not massive enough to claim it as a Miyake event. Next, I calculated my averaged results using the same formulae [6], [7], and [8] obtained from Ward, G. K., & Wilson, S. R. (1978).

Table 2: All measured Δ14C from my batch of duplicates (AD 1275-1283), as well as the averaged Δ14C for each date. Again, the chi-square test was run on all measurements and they were all valid, as the t-test results are all under the threshold of 3.84 for two samples.

	Δ14C (‰)		Δ14C (‰)	T-test	Chi-square test
Year CE	**Batch 1**	**Batch 2**	**Averaged**	**0<t<3.84**	**Pass/Fail**
1275	-17.66	-11.65	-14.46	1.76	Pass
1276	-11.64	-15.08	-13.56	1.60	Pass
1277	-14.47	-12.62	-13.44	1.60	Pass
1278	-15.44	-10.77	-12.86	1.60	Pass
1279	-10.28	-12.37	-11.29	1.67	Pass
1280	-8.18	-11.01	-9.66	1.56	Pass
1281	-10.02	-13.10	-11.34	1.63	Pass
1282	-12.61	-9.65	-11.31	1.55	Pass
1283	-8.66	-10.02	-9.44	1.57	Pass

For the second candidate event in AD 1279, the data have not been reproduced by any renowned labs, only proposed by ETH. So, our averaged data were plotted as shown in *Figure 13* below and investigated.

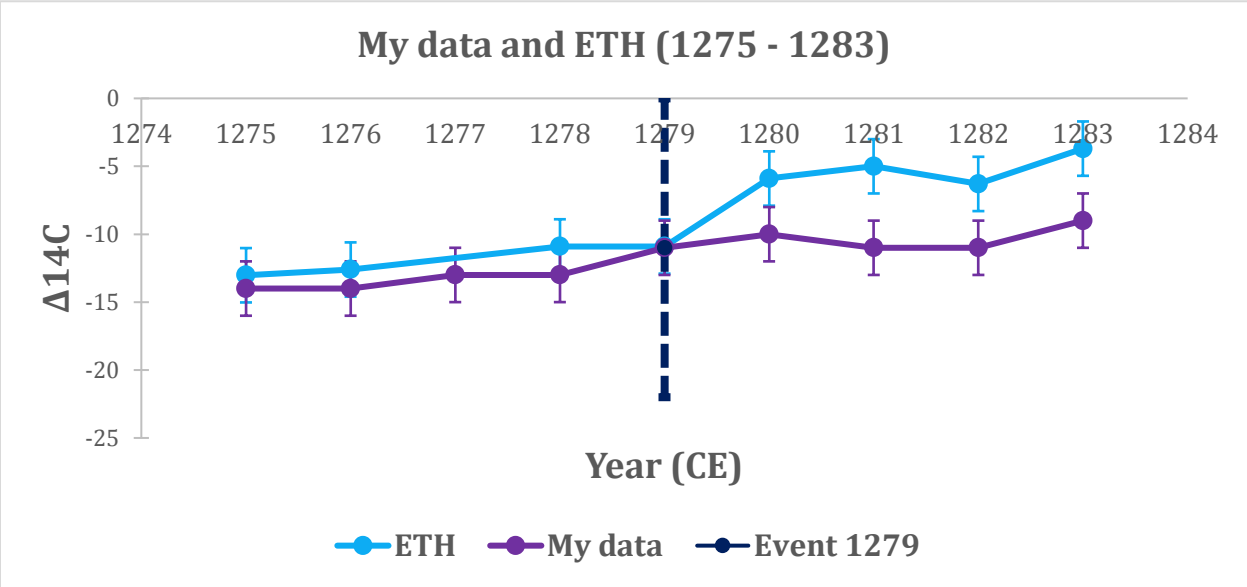

Figure 13: This graph shows my measured data from AD 1275 to 1283, as well as that of ETH for the same time period. These data seem to be even more compatible with each other than the previous batch for the years preceding the candidate event AD 1279 represented in a dashed blue line.

Although the data above seem to drift away from one another after AD 1279, they all passed the chi-square test. The rise of $\Delta^{14}C$ in AD 1279 is only about 2‰ in one year for my data. That is not powerful enough, especially compared to the AD 775 and 994 Events which increase by ~12‰ in a single-year period (Miyake et al., 2012). Once again, like the alleged AD 1054 Event, my data do not appear to substantiate any dramatic rise around AD 1279.

To illustrate, I put both proven Miyake Events (AD 775 and 994), both candidate events (AD 1054 and AD 1279), and the Carrington Event all on the same plot to discuss in this section.

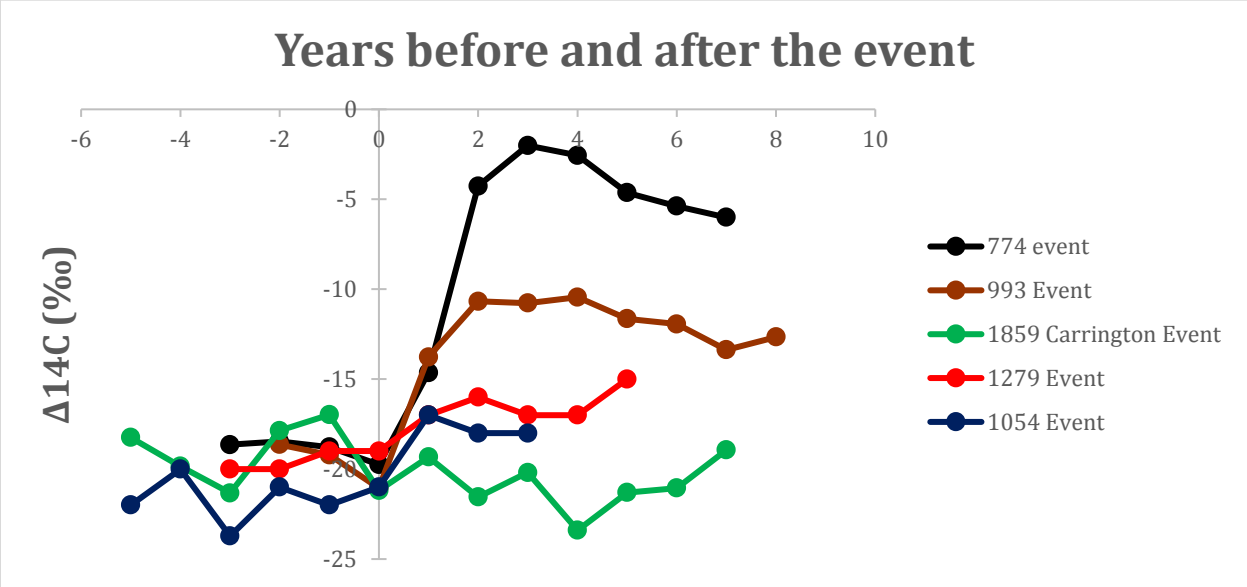

Figure 14: In this graph, two proven Miyake Events (775 and 994), one proven solar event (Carrington) and two candidate Miyake Events (1054 and 1279) have been plotted together in order to compare their trend.

As seen in the figure above, these huge spikes in black and brown represent two Miyake Events that were discovered in 2012 and 2013 (Miyake et al., 2012). Indeed, these two events seem to increase way more significantly than the two candidates that were studied in this project (blue and red). In green is the $\Delta^{14}C$ trend for the Carrington Event, which was witnessed as a solar event, although it left no imprint in the tree-ring archives.

Limitations

Radiocarbon dating is a very precise technique; however, it still suffers certain drawbacks. For instance, combining radiocarbon measurements with solar activity, especially with the International Sunspot Number (ISN) can help us understand if solar events are happening during solar minima (few sunspots) or solar maxima (numerous sunspots), however for the events in AD 1054 and AD 1279, there is no available ISN data to go through (Brehm et al., 2021). In fact, the observation of solar activity through sunspot number only covers the last 400 years (Brehm et al., 2021).

In addition, no historical sighting has been recorded for an event happening in AD 1279 which would have made the search for an origin way less complicated; whereas the AD 1054 event has potentially been linked with a supernova, SN1054 to be exact, which left behind the Crab Nebula (a supernova remnant), but that event would have been the very first rise in $\Delta^{14}C$ from a supernova, especially keeping in mind the fluctuations caused by the Schwabe Cycle (Dee et al., 2017; Menjo et al., 2005).

Thus, looking at my results again, there is no evidence of a radiocarbon spike in AD 1054 nor in AD 1279. In comparison with the AD 775 and AD 994 Miyake Events, the radiocarbon trend

is not nearly similar. These results refute the claims of Brehm et al. (2021), and indicate that there hasn't been a large single-year event since AD 994. This leads to think that the rate of occurrence of Miyake Events could have been overestimated. If that is indeed the case, does that mean a Miyake Event is coming soon?

Hazard Preparedness

One thousand years after the occurrence of the Miyake Events, the Earth went through the largest geomagnetic storm ever recorded: the Carrington Event (Cannon P.S., 2013; Scifo et al., 2019). In the beginning of September 1859, aurorae could be seen at the poles, in Europe, and all the way to the tropics and the Caribbean (Cannon P.S., 2013). It must have been phenomenal. But unfortunately, that's not all that happened. Although the Carrington Event didn't show a rise in $\Delta^{14}C$ (Scifo et al., 2019; Stuiver et al., 1998), telephone communication and telegraphs were disrupted and power blackouts for several hours were recorded (Cannon P.S., 2013). However, we should be prepared for much worse (Hapgood., 2012), because the most important question is not "if" highly energetic cosmic events will happen but "when?" (Cannon P.S., 2013).
The crux of this matter is, if these smaller solar storms were capable of such damage, what would the recurrence of a Miyake Event do? It would, as expected, prove disastrous to our highly electronic society (Hapgood., 2012; Dee et al., 2017; Brehm et al., 2021). In fact, UK National Grid suggested that a Carrington Event today would leave regions without power for several months; others predict a wide-scale disruption with ripple effects that would last for years to come along with an economic impact of several trillion dollars (Hapgood., 2012).

Now logically, people near the surface would have a slightly lower impact than, for instance, passengers in an airplane and its crew members. To illustrate, such an event would strike people with a dose of up to 20 mSv, which is significantly above the annual limit (of 1 mSv) for members of the public from a planned exposure, and about three times as high as the dose received from a CT scan of the chest (Cannon P.S., 2013). This would consequently increase cancer risk of 1 in 1,000 for each person exposed, taking into consideration the lifetime risk of cancer of 30% (Cannon P.S., 2013). In addition to this, the high-frequency communications for long-distance aircraft will also be damaged, which will likely be inoperable for several days during a solar superstorm (Cannon P.S., 2013.

So, if we cannot stop these events from happening, how can we avoid such drastic consequences? Using X-ray space telescopes, or satellite missions like STEREO, could help us monitor the sun as well as to detect emissions in space, which will give us some insight on the power carried by stellar winds, CMEs, SPEs, and other highly energetic events (Hapgood., 2012), as well as their rate of occurrence. However, neither SPEs nor flares can currently be forecasted, and they only take eight minutes to get to us (Cannon P.S., 2013); but it is important to point out that the recurrence statistics of an event similar in magnitude to the Carrington Event is poor but improving (Cannon P.S., 2013). In fact, the 95% confidence of interval for such an event ranges from 2 years to 300 years (Cannon P.S., 2013). Some improvements in the communication

infrastructure has already taken place. For instance, replacing copper wires by optical fibers in telephone systems has proven to be more resilient to space weather events (Cannon P.S., 2013).

Future Directions

To pursue radiocarbon measurements further, another cosmogenic nuclide (beryllium-10) can be used also as proxy to study short-term solar variability such as the 11-year Schwabe Cycle (Nagaya et al., 2012). In fact, the beryllium-10 concentration measured in ice cores indicates changes in the rate of production of cosmic rays more directly than carbon-14, and that is because beryllium-10 attaches itself to aerosols after production and immediately falls on earth's surface (Nagaya et al., 2012). This means that carbon-14 and beryllium-10 can be used together to trace past solar activity. However, a lot of complications arise when trying to date beryllium-10 in ice cores. For instance, the accumulation process of beryllium-10 is affected by climatic and regional effects (Nagaya et al., 2012), leading to weather-induced noise, and low temporal resolution (Brehm et al., 2021). Thus, measuring beryllium-10 concentrations is not easy, but it can be used contemporarily along with radiocarbon measurements to find simultaneous peaks in their data, indicating an increase in cosmic ray production and maybe even indicating the occurrence of some cosmic events.

In addition, to deepen our understanding about the Miyake Events (or other rises in radiocarbon), their rate of occurrence and their magnitude, a closer look at the International Calibration Curve (IntCal) could be of great help. Year-to-year measurements can be a way to obtain a pattern or at least a clearer idea behind the cause of those events. In fact, the IntCal is made up of atmospheric data trapped in tree-rings mostly in 10-year blocks. So, to discover more of these rapid 1-year events, we really need much more investments in getting new data.

Another way to look deeper into cosmic events, and more particularly solar events is to create solar models which, using the radiocarbon concentration inside tree rings, could estimate the radiocarbon produced in Earth's upper atmosphere, and give us some insight into the power and intensity of such cosmic events (Brehm et al., 2021). Furthermore, three approaches can be taken to minimize the risk of those events e.g. computer modelling to understand the risks of each cosmic event, implementing the appropriate engineering and hardware solutions like optic fibers as well as installing geomagnetic-resistant devices, and finally implementing forecasts and operational procedures when severe-risk events will occur, which are as crucial as terrestrial weather events (Cannon P.S., 2013).

Conclusion

To conclude, the two candidate events in AD 1054 and AD 1279 showed only a gentle rise slightly above background for both claims, but nothing distinctive that would indicate the presence of a Miyake event. Considering only our lab and ETH measured the AD 1279 candidate, it would be useful to obtain more annual data for this period. Also, by comparison, the proven Miyake Events in AD 775 and AD 994 were way more distinguishable than the normal annual fluctuations

that we see in the radiocarbon data. There is a lot we don't know about those events but ETH needs to be careful as to what they consider a threat to society, and what can be considered as just a normal shift in radiocarbon reservoirs. Thus, more data and better risk management can be of great help in regards to space weather events like computer modeling for solar activity, forecasting procedures and implementing geomagnetic-resistant technologies.

Literature

Bogino, S. (2014). The centenary pluviometer: a pioneer dendrochronological study in South America. *Dendrochronologia*, *32*(1), 52-54.

Bolles D., (2021). A Super Solar Flare. NASA Science Share the science [Accessed on 10/07/2021 from https://science.nasa.gov/science-news/science-at-nasa/2008/06may_carringtonflare/]

Brehm N., Beyliss A., et al., 2021. Eleven-year solar cycles over the last millennium revealed by radiocarbon in tree rings

Brothwell, D. R., & Pollard, A. M. (Eds.). (2001). *Handbook of archaeological sciences* (p. 762). J. Wiley.

Büntgen, U., Wacker, L., Galván, J. D., Arnold, S., Arseneault, D., Baillie, M., ... & Young, G. H. (2018). Tree rings reveal globally coherent signature of cosmogenic radiocarbon events in 775 and 993 CE. Nature communications, 9(1), 1-7.

Cannon, P. S. (2013). Extreme space weather—A report published by the UK Royal Academy of Engineering. *Space Weather*, *11*(4), 138-139.

Chai, Y. T., & Zou, Y. C. (2015). Searching for events in Chinese ancient records to explain the increase in 14C from AD 774–775 and AD 993–994. Research in Astronomy and Astrophysics, 15(9), 1504.

Cliver, E. W., Tylka, A. J., Dietrich, W. F., & Ling, A. G. (2014). On a solar origin for the cosmogenic nuclide event of 775 AD. The Astrophysical Journal, 781(1), 32.

Craig, H. (1957). The natural distribution of radiocarbon and the exchange time of carbon dioxide between atmosphere and sea. *Tellus*, *9*(1), 1-17.

Damon, P. E., & Linick, T. W. (1986). Geomagnetic-heliomagnetic modulation of atmospheric radiocarbon production. *Radiocarbon*, *28*(2A), 266-278.

Damon, P. E., Long, A., & Wallick, E. I. (1973). On the magnitude of the 11-year radiocarbon cycle. *Earth and Planetary Science Letters*, *20*(3), 300-306.

De Jong, A. F. M. (1981). Natural 14 C variations.

Dee, M. W., Palstra, S. W. L., Aerts-Bijma, A. T., Bleeker, M. O., De Bruijn, S., Ghebru, F., ... & Meijer, H. A. J. (2020). Radiocarbon dating at Groningen: New and updated chemical pretreatment procedures. Radiocarbon, 62(1), 63-74.

Dee, M., Pope, B., Miles, D., Manning, S., & Miyake, F. (2017). Supernovae and single-year anomalies in the atmospheric radiocarbon record. *Radiocarbon*, *59*(2), 293-302.

Douglass, A. E. (1941). Crossdating in dendrochronology. Journal of Forestry, 39(10), 825-831.

Gaisser, T. K., Engel, R., & Resconi, E. (2016). *Cosmic rays and particle physics*. Cambridge University Press

Global Monitoring Laboratory. 2021. The Technical Details: Chemistry Composition of an Atom. NOAA Research [Accessed on 10/02/2021 from https://gml.noaa.gov/ccgg/isotopes/chemistry.html]

Guibal, F., & Guiot, J. (2021). Dendrochronology. In *Paleoclimatology* (pp. 117-122). Springer, Cham.

Güttler, D., Adolphi, F., Beer, J., Bleicher, N., Boswijk, G., Christl, M., ... & Wunder, J. (2015). Rapid increase in cosmogenic 14C in AD 775 measured in New Zealand kauri trees indicates short-lived increase in 14C production spanning both hemispheres. *Earth and Planetary Science Letters*, *411*, 290-297.

Hackens, T. (1995). 14C methods and applications: a symposium dedicated to Ingrid Olsson on the occasion of a birthday.
Hakozaki, M., Miyake, F., Nakamura, T., Kimura, K., Masuda, K., & Okuno, M. (2018). Verification of the annual dating of the 10th Century Baitoushan Volcano eruption based on an AD 774–775 radiocarbon spike. *Radiocarbon*, *60*(1), 261-268.

Hambaryan, V. V., & Neuhäuser, R. (2013). A Galactic short gamma-ray burst as cause for the 14C peak in AD 774/5. *Monthly Notices of the Royal Astronomical Society*, *430*(1), 32-36.

Hapgood. (2012. Prepare for the coming space storm.

Jeong, J., Barichivich, J., Peylin, P., Haverd, V., McGrath, M. J., Vuichard, N., ... & Luyssaert, S. (2020). Using the International Tree-Ring Data Bank (ITRDB) records as century-long benchmarks for land-surface models. *Geoscientific Model Development Discussions*, 1-45.

Jull, A. T., Panyushkina, I. P., Lange, T. E., Kukarskih, V. V., Myglan, V. S., Clark, K. J., ... & Leavitt, S. W. (2014). Excursions in the 14C record at AD 774–775 in tree rings from Russia and America. *Geophysical Research Letters*, *41*(8), 3004-3010.

Kitagawa, H., & van der Plicht, J. (1998). Atmospheric radiocarbon calibration to 45,000 yr BP: Late glacial fluctuations and cosmogenic isotope production. Science, 279(5354), 1187-1190. https://doi.org/10.1126/science.279.5354.1187

Kovaltsov, G. A., Mishev, A., & Usoskin, I. G. (2012). A new model of cosmogenic production of radiocarbon 14C in the atmosphere. *Earth and Planetary Science Letters*, *337*, 114-120.

Kromer, B. (2009). Radiocarbon and dendrochronology. Dendrochronologia, 27(1), 15-19.

Liu, Y., Zhang, Z. F., Peng, Z. C., Ling, M. X., Shen, C. C., Liu, W. G., ... & Sun, W. (2014). Mysterious abrupt carbon-14 increase in coral contributed by a comet. Scientific reports, 4(1), 1-4.

Machmudah, S., Kanda, H., & Goto, M. (2017). Hydrolysis of biopolymers in near-critical and subcritical water. In *Water Extraction of Bioactive Compounds* (pp. 69-107). Elsevier.

Mekhaldi, F., Muscheler, R., Adolphi, F., Aldahan, A., Beer, J., McConnell, J. R., ... & Woodruff, T. E. (2015). Multiradionuclide evidence for the solar origin of the cosmic-ray events of AD 774/5 and 993/4. *Nature communications*, *6*(1), 1-8.

Melott, A. L., & Thomas, B. C. (2012). Causes of an AD 774–775 14 C increase. Nature, 491(7426), E1-E2.

Menjo, H., Miyahara, H., Kuwana, K., Masuda, K., Muraki, Y., & Nakamura, T. (2005). Possibility of the detection of past supernova explosion by radiocarbon measurement. In *29th International Cosmic Ray Conference (ICRC29), Volume 2* (Vol. 2, p. 357).

Miyake, F., Nagaya, K., Masuda, K., & Nakamura, T. (2012). A signature of cosmic-ray increase in AD 774–775 from tree rings in Japan. *Nature*, *486*(7402), 240-242.

Miyake, F., Masuda, K., & Nakamura, T. (2013). Another rapid event in the carbon-14 content of tree rings. *Nature communications*, *4*(1), 1-6.

Nagaya, K., Kitazawa, K., Miyake, F., Masuda, K., Muraki, Y., Nakamura, T., ... & Matsuzaki, H. (2012). Variation of the Schwabe cycle length during the grand solar minimum in the 4th century BC deduced from radiocarbon content in tree rings. Solar Physics, 280(1), 223-236.

NASA. (2020). What is space radiation? NASA Space Radiation Analysis Group, Johnson Space Center. <https://srag.jsc.nasa.gov/SpaceRadiation/What/What.cfm> [Accessed 04/11/2021]

NASA GMS. (2009). Keeping Up With Carbon. [Accessed on 10/02/2021 from https://svs.gsfc.nasa.gov/10498]

NASA Goddard Space Flight Center. Cosmic Ray. (2017). [Accessed on 10/02/2021 from https://imagine.gsfc.nasa.gov/science/toolbox/cosmic_rays1.html]

National Oceanic and Atmospheric Administration.space Weather Prediction Center. (2022). Coronal Mass Ejections [Retrieved on 20/01/2022 from https://www.swpc.noaa.gov/phenomena/coronal-mass-ejections]

NOAA. (2022). https://www.swpc.noaa.gov/phenomena/coronal-mass-ejections

Pavlov, A. K., Blinov, A. V., Vasilyev, G. I., Vdovina, M. A., Volkov, P. A., Konstantinov, A. N., & Ostryakov, V. M. (2013). Gamma-ray bursts and the production of cosmogenic radionuclides in the Earth's atmosphere. *Astronomy Letters*, *39*(9), 571-577.

Povinec, P. P., Litherland, A. E., & von Reden, K. F. (2009). Developments in radiocarbon technologies: from the Libby counter to compound-specific AMS analyses. Radiocarbon, 51(1), 45-78.

Ramsey Bronk, C. (2008). Radiocarbon dating: revolutions in understanding. Archaeometry, 50(2), 249-275.

Reddy F., 2015 NASA [Retrieved on 27/01/2022 from https://www.nasa.gov/feature/goddard/2021/nasa-missions-unmask-magnetar-eruptions-in-nearby-galaxies]

Riebeek H, .2011. The Carbon Cycle. NASA The Earth Observatory. [Accessed on 10/01/2022 from https://www.earthobservatory.nasa.gov/features/CarbonCycle]

Rubin, M., Likins, R. C., & Berry, E. G. (1963). On the validity of radiocarbon dates from snail shells. *The Journal of Geology*, *71*(1), 84-89.

Scharpenseel, H. W., Becker-Heidmann, P., Neue, H. U., & Tsutsuki, K. (1989). Bomb-carbon, 14C-dating and 13C—measurements as tracers of organic matter dynamics as well as of morphogenetic and turbation processes. Science of the Total Environment, 81, 99-110.

Scifo, A., Kuitems, M., Neocleous, A., Pope, B. J. S., Miles, D., Jansma, E., ... & Dee, M. W. (2019). Radiocarbon production events and their potential relationship with the schwabe cycle. Scientific reports, 9(1), 1-8.

Sensuła, B. M., Pazdur, A., & Marais, M. F. (2011). First application of mass spectrometry and gas chromatography in investigation of α-cellulose hydrolysates: the influence of climate changes on glucose molecules in pine tree-rings. Rapid Communications in Mass Spectrometry, 25(4), 489-494.

Shibata, K., Isobe, H., Hillier, A., Choudhuri, A. R., Maehara, H., Ishii, T. T., ... & Nogami, D. (2013). Can superflares occur on our Sun?. Publications of the Astronomical Society of Japan, 65(3), 49.

Sjostrom, E. (1981). The structure of wood. *Wood chemistry: fundamentals and applications.*, 1-20.

Stuiver, M. (1961). Variations in radiocarbon concentration and sunspot activity. *Journal of Geophysical Research*, *66*(1), 273-276.

Stuiver, M., Reimer, P. J., & Braziunas, T. F. (1998). High-precision radiocarbon age calibration for terrestrial and marine samples. *radiocarbon*, *40*(3), 1127-1151.

Terrasi, F., Marzaioli, F., Buompane, R., Passariello, I., Porzio, G., Capano, M., ... & Usoskin, I. (2020). Can the 14C production in 1055 CE be affected by SN1054?. *Radiocarbon*, *62*(5), 1403-1418.

Thomas, B. C., Melott, A. L., Arkenberg, K. R., & Snyder, B. R. (2013). Terrestrial effects of possible astrophysical sources of an AD 774-775 increase in 14C production. *Geophysical research letters*, *40*(6), 1237-1240.

Usoskin, I. G., Koldobskiy, S. A., Kovaltsov, G. A., Rozanov, E. V., Sukhodolov, T. V., Mishev, A. L., & Mironova, I. A. (2020). Revisited reference solar proton event of 23 February 1956: assessment of the cosmogenic-isotope method sensitivity to extreme solar events. Journal of Geophysical Research: Space Physics, 125(6), e2020JA027921

Usoskin, I. G., & Kovaltsov, G. A. (2015). The carbon-14 spike in the 8th century was not caused by a cometary impact on Earth. Icarus, 260, 475-476

Usoskin, I. G., Kromer, B., Ludlow, F., Beer, J., Friedrich, M., Kovaltsov, G. A., ... & Wacker, L. (2013). The AD775 cosmic event revisited: the Sun is to blame. Astronomy & Astrophysics, 552, L3.

Wang, F. Y., Li, X., Chernyshov, D. O., Hui, C. Y., Zhang, G. Q., & Cheng, K. S. (2019). Consequences of Energetic Magnetar-like Outbursts of Nearby Neutron Stars: 14C Events and the Cosmic Electron Spectrum. *The Astrophysical Journal*, *887*(2), 202.

Ward, G. K., & Wilson, S. R. (1978). Procedures for comparing and combining radiocarbon age determinations: a critique. *Archaeometry*, *20*(1), 19-31.

Appendices

ETH Annual Data 1052 averages:

Year (cal BP)	Year (CE)	$\Delta^{14}C$	$\Delta^{14}C$ (±)
868	1082	-13.10	1.70
869	1081	-14.45	1.13
870	1080	-13.30	1.70
871	1079	-9.20	1.70
872	1078	-10.55	1.13
873	1077	-8.50	1.70
874	1076	-9.50	1.70
875	1075	-9.20	1.13
876	1074	-12.30	1.70
877	1073	-10.30	1.70
878	1072	-8.25	1.13
879	1071	-7.40	1.70
880	1070	-9.80	1.70
881	1069	-8.45	1.13
882	1068	-7.80	1.70
883	1067	-5.55	1.13
884	1066	-8.90	1.70
885	1065	-9.90	1.70
886	1064	-7.50	1.13
887	1063	-7.40	1.70
888	1062	-8.60	1.70
889	1061	-6.90	1.13
890	1060	-8.90	1.70
891	1059	-6.00	1.70
892	1058	-8.55	1.13
893	1057	-8.00	1.70
894	1056	-4.90	1.60
895	1055	-2.85	1.13
896	1054	-3.60	1.60
897	1053	-4.80	1.60
898	1052	-10.55	1.13
899	1051	-8.60	1.60
900	1050	-7.50	1.60

901	1049	-9.00	1.13
908	1048	-13.20	1.60
909	1047	-10.10	1.60
910	1046	-12.30	1.60
911	1045	-11.20	1.60
912	1044	-11.70	1.60
913	1043	-11.10	1.60
914	1042	-8.00	1.60
915	1041	-11.00	1.60
916	1040	-9.50	1.60
917	1039	-11.50	1.60
918	1038	-10.30	1.60
919	1037	-14.50	1.60
920	1036	-10.60	1.70
921	1035	-13.38	1.17
922	1034	-12.50	1.70
923	1033	-13.00	1.70
924	1032	-14.73	1.17
925	1031	-12.50	1.70
926	1030	-11.90	1.60
927	1029	-14.58	1.17
928	1028	-18.20	1.70

ETH Annual Data 1279 Averages

Year (cal BP)	Year (CE)	$\Delta^{14}C$	$\Delta^{14}C$ (±)
640	1310	-1.1	1.9
642	1308	-4.0	1.9
643	1307	0.7	2.0
644	1306	1.6	1.3
645	1305	-2.9	1.9
647	1303	-3.2	1.3
648	1302	-4.3	1.9
649	1301	-3.6	2.0
650	1300	-2.5	1.3
651	1299	-3.2	1.9
652	1298	-5.5	1.9
653	1297	-4.6	1.3
654	1296	-7.9	1.9

655	1295	-6.1	1.9
656	1294	-6.1	1.3
657	1293	-4.9	2.4
658	1292	-5.7	2.4
659	1291	-4.7	2.4
660	1290	-6.7	2.3
661	1289	-7.0	2.3
662	1288	-4.1	2.4
663	1287	-5.7	2.4
664	1286	-10.0	2.3
665	1285	-7.2	2.3
666	1284	-9.1	2.3
667	1283	-3.7	2.4
668	1282	-6.3	2.4
669	1281	-5.0	2.4
670	1280	-5.9	2.4
671	1279	-10.9	2.3
672	1278	-10.9	2.3
674	1276	-12.6	1.4
675	1275	-13.0	1.5
676	1274	-12.1	1.8
677	1273	-13.0	2.1
678	1272	-12.8	1.8
679	1271	-11.9	2.1
680	1270	-10.6	1.8
681	1269	-15.8	2.1
682	1268	-15.1	1.8
683	1267	-15.5	2.1
684	1266	-13.0	1.8
685	1265	-15.9	2.1
686	1264	-15.4	1.8
687	1263	-16.7	2.1
688	1262	-18.9	1.8
689	1261	-15.0	2.1
690	1260	-14.2	1.8
691	1259	-16.5	2.1
692	1258	-19.8	1.8
693	1257	-18.6	2.1
694	1256	-14.2	1.8

695	1255	-12.3	2.2
696	1254	-15.4	1.8
697	1253	-18.1	2.1
698	1252	-15.0	2.0
699	1251	-17.9	2.1
700	1250	-15.9	1.8
701	1249	-16.5	2.1

Eastoe Annual Data: AD 1054 candidate

Year (AD)	$\Delta^{14}C$ (‰)	Error (1σ)
1049	-14.6	1.8
1050	-10.4	1.9
1051	-10.9	1.9
1052	-14.1	1.9
1053	-5.7	2.5
1054	-7.3	1.9
1055	-0.5	1.9
1056	0.8	2.0
1057	-4.6	1.9

Terrasi Annual Data: AD 1054 candidate

Year (CE)	Δ14C	±	Δ14C	±	Δ14C	±
1049	**-9.7**	**2**	**-9.6**	**1.4**		
1050	**-7.2**	**2**	**-8.2**	**1.4**	**-10.3**	**3.1**
1051	**-3.1**	**2**	**-5.7**	**1.4**	**-10.5**	**3.9**
1052	**-7.4**	**2**	**-5.9**	**1.4**	**-4.7**	**4.4**
1053	**-7.8**	**2**	**-6.3**	**1.4**	**-0.1**	**3.9**
1054	**-0.9**	**2.1**	**-2.5**	**1.5**	**-0.1**	**3.9**
1055	**2.1**	**2.2**	**1.2**	**1.5**	**3.1**	**3.6**
1056	**-1.6**	**2.2**	**-2**	**1.5**	**-8.4**	**4.5**
1057	**-3.1**	**2.1**	**-3.8**	**1.5**	**0.4**	**3.7**

Menjo Data AD 1054 candidate

Year CE	$\Delta^{14}C$	±
1050	-11.5	2.8
1052	-7.8	2.8
1054	-2.2	2.8
1056	-7.5	2.8
1058	-8.4	2.8

1060	-7.1	2.8
1062	-10.1	2.8
1064	-13.3	2.8

Chi-square tests:

Chi-square test (Me vs ETH) 1049-1057				
Year (CE)	**14C age**	**±**	**T-test**	**Chi square**
1049	-8.52	0.98	0.76	Pass
1050	-6.52	1.25	0.95	Pass
1051	-8.67	1.09	0.003	Pass
1052	-9.45	0.98	3.92	Fail
1053	-5.66	1.23	0.74	Pass
1054	-4.54	1.23	0.88	Pass
1055	-2.64	0.98	0.14	Pass
1056	-4.16	1.25	0.55	Pass
1057	-5.90	1.30	3.63	Pass

Chi-square test (Me vs ETH-2) 1049-1057				
Year (CE)	**14C age**	**±**	**T-test**	**Chi square**
1049	-9.0	1.0	1.5	Pass
1050	-10.0	1.0	10.3	Fail
1051	-9.0	1.0	0.022	Pass
1052	-7.0	1.0	0.3	Pass
1053	-8.0	1.0	0.4	Pass
1054	-9.0	1.0	3.9	Fail
1055	-4.0	1.0	1.2	Pass
1056	-3.0	1.0	0.1	Pass
1057	-3.0	1.0	0.004	Pass

Chi-square test (Me vs Terrasi)				
Year (CE)	**Averaged D14C**	**±**	**T-test**	**Chi-square**
1049	-9.4	0.89	1.8	Pass
1050	-7.4	0.89	1.8	Pass
1051	-6.52	0.88	3.4	Pass
1052	-6.22	0.97	0.02	Pass
1053	-6.46	0.97	0.1	Pass
1054	-2.85	1	3.32	Pass
1055	0.73	1.01	2.5	Pass

1056	-2.51	1.02	0.08	Pass
1057	-3.13	1	0.01	Pass

Chi-square test (Me vs Eastoe)				
Year (CE)	**14C age**	**±**	**T-test**	**Chi square**
1049	-11.2	1.3	7.978	Fail
1050	-7.8	1.4	3.832	Pass
1051	-9.5	1.2	0.826	Pass
1052	-10.3	1.4	8.622	Fail
1053	-6.5	1.6	0.165	Pass
1054	-6.7	1.4	0.222	Pass
1055	-1.2	1.4	0.296	Pass
1056	-1.1	1.4	1.805	Pass
1057	-3.8	1.4	0.336	Pass

Chi square test (All 1049-1057)				
Year	**14C age**	**±**	**t-test**	**Chi-square**
1049	-10	1	9.3	Fail
1050	-8	1	4	Pass
1051	-8	1	8.3	Fail
1052	-8	1	14.7	Fail
1053	-6	1	0.9	Pass
1054	-4	1	7.6	Pass
1055	-0.3	0.8	5.6	Pass
1056	-2.6	0.8	5	Pass
1057	-4.4	0.8	6.1	Pass

Chi-square test Me vs ETH 1275-1283				
Year CE	**D14C avg**	**±**	**t-test**	**Chi-square**
1275	-13.36	1.2	0.2	Pass
1276	-13.06	1.15	0.329	Pass
1277				
1278	-12.1	1.51	0.475	Pass
1279	-10.96	1.51	0.001	Pass
1280	-8.32	1.54	1.722	Pass
1281	-8.54	1.54	3.689	Pass
1282	-9.07	1.54	2.263	Pass
1283	-6.83	1.54	2.878	Pass

Chi-square test (All 1279)				
Year CE	D14C avg	±	t-test	Chi-square
1275	-11.09	1.03	13.6	Fail
1276	-12.51	0.98	1.2	Pass
1277	-11.84	1.34	0.609	Pass
1278	-12.5	1.2	0.7	Pass
1279	-8.17	1.16	8.3	Fail
1280	-9.12	1.14	2.3	Pass
1281	-7.3	1.17	5.2	Pass
1282	-8.66	1.17	2.4	Pass
1283	-5.43	1.17	4.9	Pass